Calcif. Tiss. Res. 25, 209–216 (1978)

Calcified
Tissue Research

Laboratory Investigations

A Thermodynamic Analysis of the Secondary Transition in the Spontaneous Precipitation of Calcium Phosphate

J.L. Meyer and E.D. Eanes

Laboratory of Biological Structure, National Institute of Dental Research, National Institutes of Health, Building 30, Room 211, Bethesda, Maryland 20014, USA

Summary. A thermodynamic analysis has been made of the secondary transition stage in the spontaneous precipitation of calcium phosphate following the amorphous–crystalline transformation. The first formed crystalline material has a solubility similar to that of octacalcium phosphate (OCP) and the computed thermodynamic solubility product remains invariant in the pH range 7.00–8.60. The duration of the secondary stage is sensitive to pH and the transition appears to occur by hydrolysis of the first formed OCP-like phase to a more basic apatitic phase with a tricalcium phosphate (TCP) stoichiometry. The crystalline material at the end of this transition has an invariant solubility product, in the pH range 7.00 to 8.60, when the TCP-like molecular formula is assumed. Changes in the solution chemistry which accompany the solid-to-solid transitions are consistent with the above conclusions. The results of this study are also consistent with those of a previous study which suggest that the stability of the amorphous calcium phosphate phase is dependent upon the instability of the solution phase with respect to OCP formation.

Key words: Thermodynamics — Kinetics — Apatite — Octacalcium phosphate — Tricalcium phosphate.

Introduction

The solution and solid state characteristics of the amorphous–crystalline transformation have been well defined (Eanes and Posner, 1965; Termine and Eanes, 1972; Boskey and Posner, 1973; Meyer and Eanes, in press). Amorphous calcium phosphate (ACP) is the first formed solid phase which, after a reproducible induction period, transforms into a microcrystalline phase with an apatitic X-ray diffraction pattern. ACP, in spite of its apparent lack of long-range order, is a definite chemical entity with demonstrated short-range structure (Betts and Posner, 1974) and an invariant thermodynamic solubility product (Meyer and Eanes, in press). ACP has a predictable life time in solution. However, its instability with respect to OCP, rather than to more basic calcium phosphate phases, best describes its subsequent transformation to a crystalline phase (Meyer and Eanes, in press). Since apatite is the crystalline material ultimately found in precipitated calcium phosphate solutions of basic pH, it appears that at least one other calcium phosphate phase must be involved. A secondary transition has been recently observed at pH 7.4 in which the intermediate phase differed from the final apatitic phase by subtle changes in crystal morphology and X-ray diffraction patterns (Eanes and Meyer, 1977). Apparent phase changes have also been observed in seeded calcium phosphate crystal growth systems (Nancollas and Tomazic, 1974).

It was the purpose of this study to investigate this secondary transformation in more detail by a thermodynamic approach. A large number of spontaneous precipitations were conducted over a wide range of pH. Sufficient data points were collected in each experiment to define precisely the duration and thermodynamic properties of the secondary stage. These results were interpreted, when possible, to demonstrate the presence or absence of well-defined crystalline calcium phosphate phases.

Materials and Methods

Subsaturated solutions of calcium phosphate were prepared by adding measured amounts of concentrated calcium nitrate (80 m*M*)

Send request for offprints to J.L. Meyer at the above address

0008–0594/78/0025–0209$01.60

and potassium dihydrogen phosphate (48 m*M*) stock solution to deionized, distilled, carbonate-free water to yield a total volume of 600 ml. Upon thermal equilibrium at 25° C, spontaneous precipitation was induced by rapidly raising the pH of the acidic solution to the desired reaction pH by the addition of the appropriate amount of concentrated (2 *M*) potassium hydroxide. The results of the experiments were unaffected by the method used for spontaneous precipitation, as determined by separate experiments, as long as the final reaction pH was quickly attained (≤1 min). The pH was maintained at the desired level, within ±0.01 pH units, by means of a Metrohm Combititrator 3-D pH stat which added the potassium hydroxide solution. The continuous trace of base consumed vs. time of reaction given by the pH stat provided an additional means of monitoring the precipitation reaction. Nitrogen gas was bubbled through the solution to prevent the uptake of carbon dioxide. All chemicals used were reagent grade and were used without further purification.

The solution concentrations of calcium and phosphate, in equilibrium with the precipitated calcium phosphate phases, were determined in 5 ml aliquots withdrawn at various time intervals. These samples were immediately (<10 s) filtered through 0.22 μm millipore filters and the resulting filtrates were analyzed for calcium and phosphate. Calcium concentrations were determined by atomic absorption spectrophotometry while phosphate concentrations were determined by the method of Murphy and Riley (1962).

Calcium phosphate was formed by spontaneous precipitation at values of pH in the range of 7.00 to 9.00. Precipitation experiments were performed at 0.20 pH unit intervals. Initial calcium and phosphate concentrations before spontaneous precipitation were approximately 10.0 and 7.0 m*M* respectively. This initial Ca/P ratio assured that sufficient calcium and phosphate would remain in solution after the initial precipitation and during the subsequent transformation stages for accurate chemical analyses. Although samples were taken for chemical analysis during the entire course of the experiments, they were taken at more frequent intervals during the post-ACP–crystalline transformation stage in order to examine this stage in more detail.

Results

Typical plots of total calcium and phosphate concentration vs. time are shown in Figures 1–3 at pH values of 7.00, 8.00, and 9.00. These 3 experiments encompassed the range of conditions used in this study. The initial sharp break in the curves indicates that the first formed ACP has converted to a crystalline calcium phosphate phase of lower solubility. A second, less pronounced, break in the solution curves is also noted at a later stage in the pH 7.00 and pH 8.00 curves. The position of the second inflection point is indicated by an arrow in Figures 1 and 2. A second inflection is not apparent in Figure 3. Although solution phosphate is sometimes seen to increase preceeding a break in the curves, i.e. Figure 2, the overall solubility of the solid phase is constantly decreasing, as will be shown later in the free energy plots. Also plotted is the continuous trace of the amount of KOH added by the pH stat to the solution to maintain constant pH. Inflections in the base uptake curves occur at the same time as those in the solution lattice ion plots.

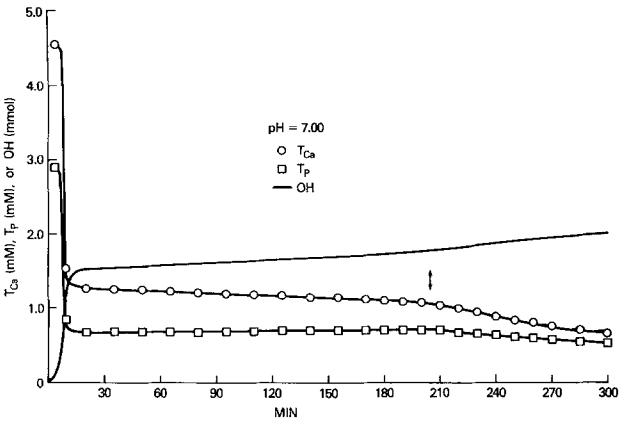

Fig. 1. Variation with time of total calcium (T_{Ca}; O), total phosphate (T_p; □), and base uptake (OH; —) for the experiment in which calcium phosphate was spontaneously precipitated at pH 7.00. Arrow signifies end of secondary transition period

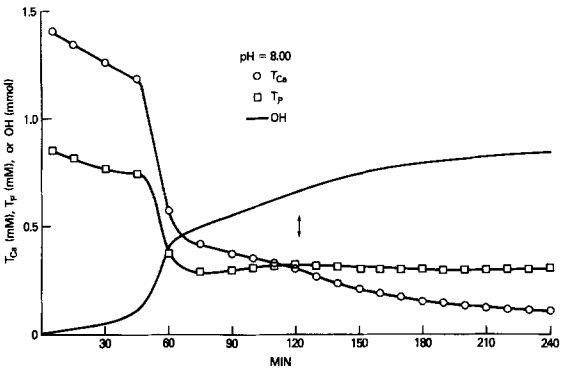

Fig. 2. Variation with time of total calcium (T_{Ca}; O), total phosphate (T_p; □), and base uptake (OH; —) for the experiment in which calcium phosphate was spontaneously precipitated at pH 8.00. Arrow signifies end of secondary transition period

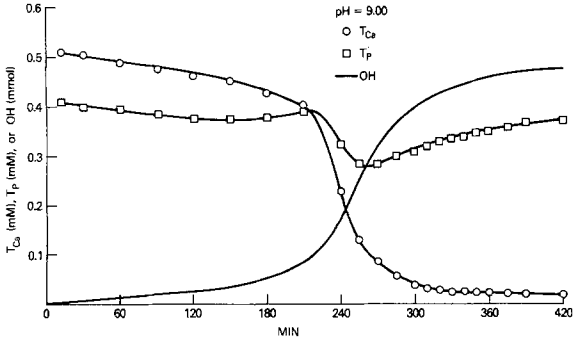

Fig. 3. Variation with time of total calcium (T_{Ca}; O), total phosphate (T_p; □) and base uptake (OH; —) for the experiment in which calcium phosphate was spontaneously precipitated at pH 9.00

Free ionic calcium and phosphate activities were calculated for all solutions in all experiments from the analytically determined total concentrations of calcium and phosphate as described earlier (Meyer and Eanes, in press). Activity products were calculated for the solution phase at each point using molecular formulas for the calcium phosphate phases: $Ca_5(PO_4)_3OH$, hydroxyapatite (HAP); $Ca_3(PO_4)_2$, tricalcium phosphate (TCP); $Ca_4H(PO_4)_3 \cdot 2.5H_2O$, octacalcium phosphate (OCP); and $CaHPO_4 \cdot 2H_2O$, dicalcium phosphate dihydrate (DCPD). The thermodynamic stabilities of the experimental solutions with respect to a solution in equilibrium with the well-defined pure crystalline phases HAP, TCP, OCP, and DCPD were determined at each point in the precipitation sequence using the equation:

$$\Delta G = -2.303RT/n \log (AP_i/AP_s)$$

where AP_i is the ionic activity product at any point in the precipitation experiment and AP_s is the thermodynamic solubility product. R and T are the ideal gas constant and absolute temperature, respectively, and n is the number of ionic terms in the activity product expression. The thermodynamic solubility products, at 25° C, used in the calculations for DCPD, TCP, and HAP were those of Gregory et al. (1970), Gregory et al. (1974) and McDowell et al. (1969), respectively. The activity coefficients and ion pair constants used in this study for the ionic activity calculations were used to compute a thermodynamic solubility product for OCP using the solubility data given by Moreno et al. (1960). The logarithm of the value so obtained was −47.33.

The ΔG calculations serve two purposes. First, when plotted vs. time, the ΔG values show how the calcium phosphate ion products in solution vary during the course of the precipitation experiments. Discontinuities in the kinetic curves signal changes that have occurred, or are about to occur, in the solid phase.

Secondly, the ΔG values indicate the thermodynamic stability of the experimental solutions compared to solutions in thermodynamic equilibrium with that particular phase. Calculated ΔG values, at or near zero, suggest the possibility that the solution phase may be in equilibrium with the solid phase for which a solubility product is known. The evidence is particularly strong if the ΔG curves consistently flatten out at this point ($\Delta G = 0$) at the beginning, or the end, of an apparent phase transition in spite of a wide variation in experimental conditions. In each of the remaining Figures a line is drawn at $\Delta G = 0$ (except for those Figures in which it would be off scale). Points above the line (ΔG negative) represent solutions less stable (i.e. supersaturated) and points below the line (ΔG positive) more stable (i.e. subsaturated) than those in thermodynamic equilibrium.

The ΔG curves are presented in two ways. First the computed ΔG values are plotted vs. time for the entire course of the precipitation starting with the formation of ACP and ending after the secondary transition had been completed. These plots are in Figures 4–7 and utilize the data obtained at pH 7.20, 7.60, 8.00, 8.40, and 8.80. The experimental data obtained at pH 7.00, 7.40, 7.80, 8.20, 8.60, and 9.00 are plotted in Figures 8–11. The experimental points in these graphs encompass only the secondary transition. The time axis is expanded and the origin is shifted such that the midpoint in the sharp break in the curve, which signals the amorphous–crystalline transition, occurs at approximately $t = 0$. The experimental data at all values of pH were not plotted both ways for simplicity.

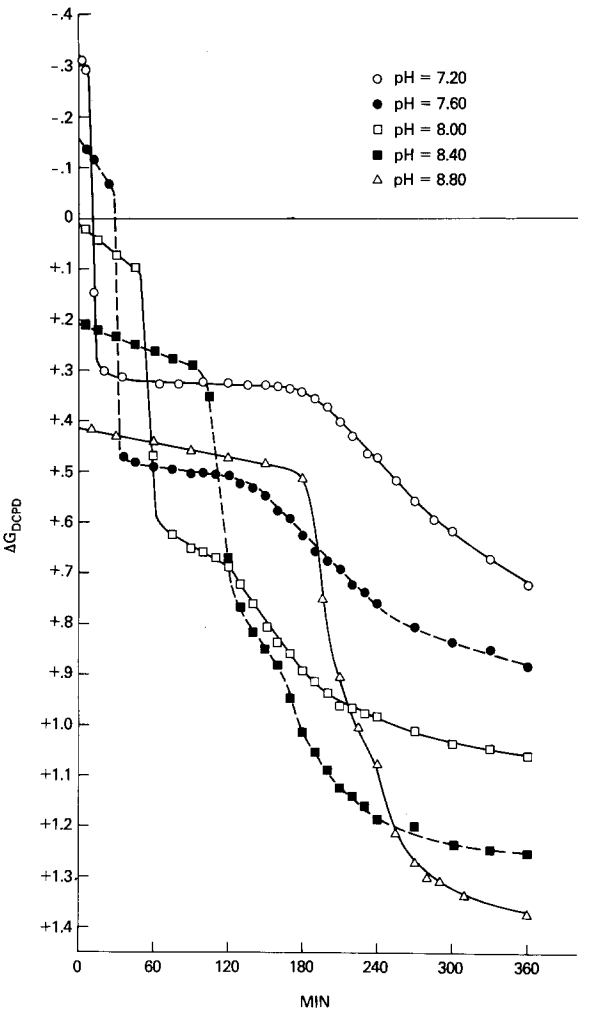

Fig. 4. The thermodynamic stability of solutions of pH 7.20, 7.60, 8.00, 8.40, and 8.80 compared to solutions in equilibrium with pure crystalline DCPD. The experiments encompass the amorphous–crystalline and the secondary transition stages

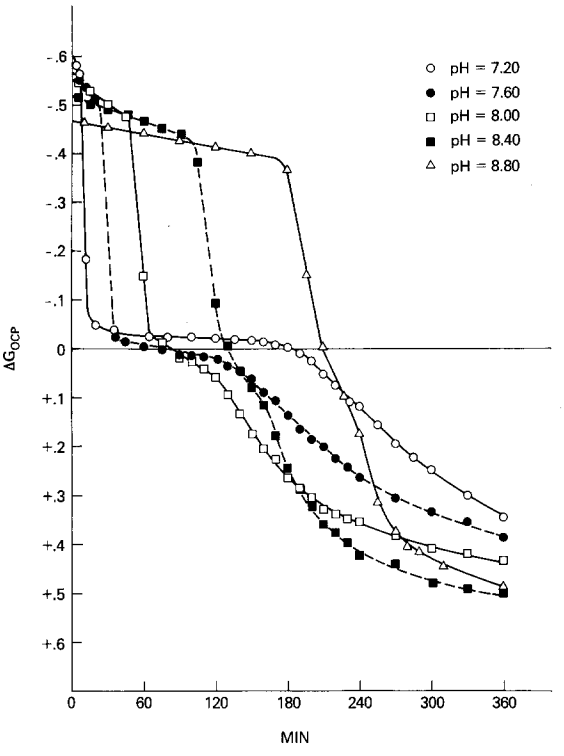

Fig. 5. The thermodynamic stability of solutions of pH 7.20, 7.60, 8.00, 8.40, and 8.80 compared to solutions in equilibrium with pure crystalline OCP. The experiments encompass the amorphous–crystalline and the secondary transition stages

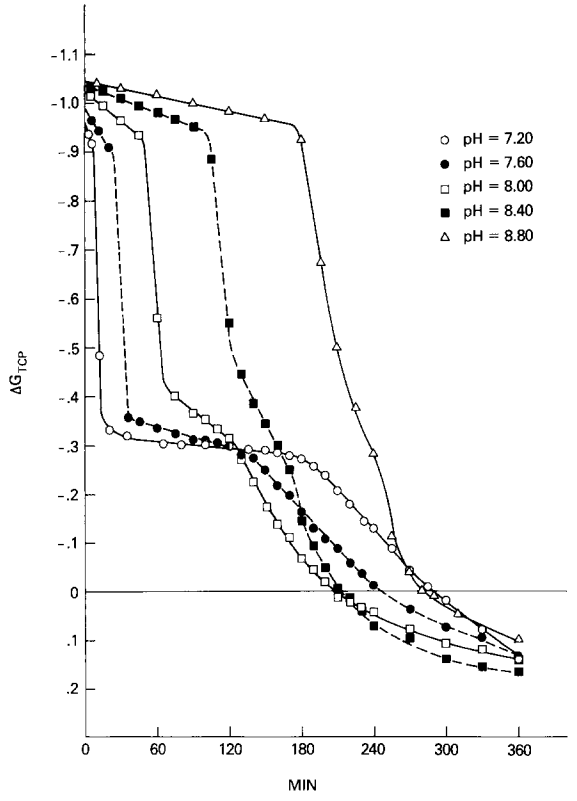

Fig. 6. The thermodynamic stability of solutions of pH 7.20, 7.60, 8.00, 8.40, and 8.80 compared to solutions in equilibrium with pure crystalline TCP. The experiments encompass the amorphous–crystalline and the secondary transition stages

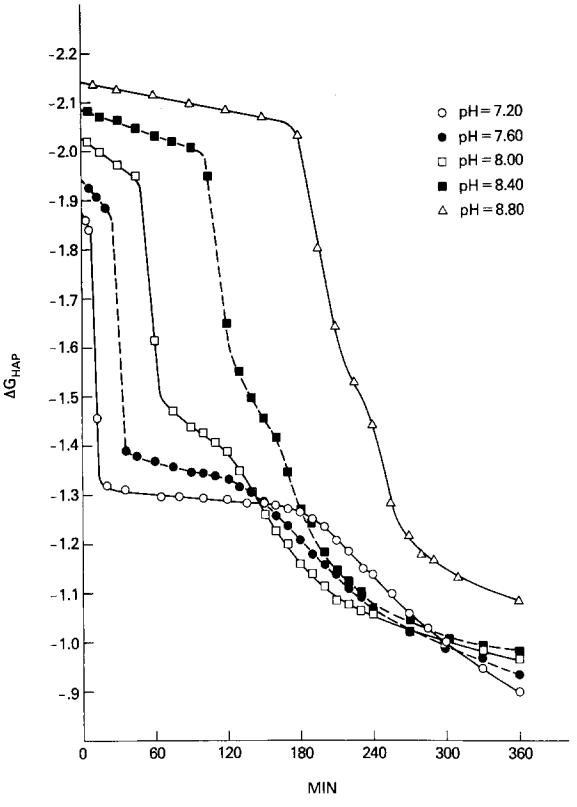

Fig. 7. The thermodynamic stability of solutions of pH 7.20, 7.60, 8.00, 8.40, and 8.80 compared to solutions in equilibrium with pure crystalline HAP. The experiments encompass the amorphous–crystalline and the secondary transition stages

Figures 4–7 show both the amorphous–crystalline transformation and the secondary transition stage. It should be noted that as the pH is increased the duration of the first stage increases whereas the secondary transition occurs more rapidly. Only in Figure 5 do the curves consistently flatten at approximately $\Delta G = 0$, suggesting the possibility that crystalline OCP may be influencing the overall solubility of the solution. Figures 8–11 exhibit the secondary stage in more detail, and show more clearly (i.e. Fig. 9) the comparability of the solution phase during the secondary transition with a solution in thermodynamic equilibrium with pure crystalline OCP. Figures 8, 10, and 11 show no such relationship with the $\Delta G = 0$ line.

Numerical data for the secondary transition are presented in Table 1. The symbols t_B and t_A are the times, in minutes, that signify the beginning and end,

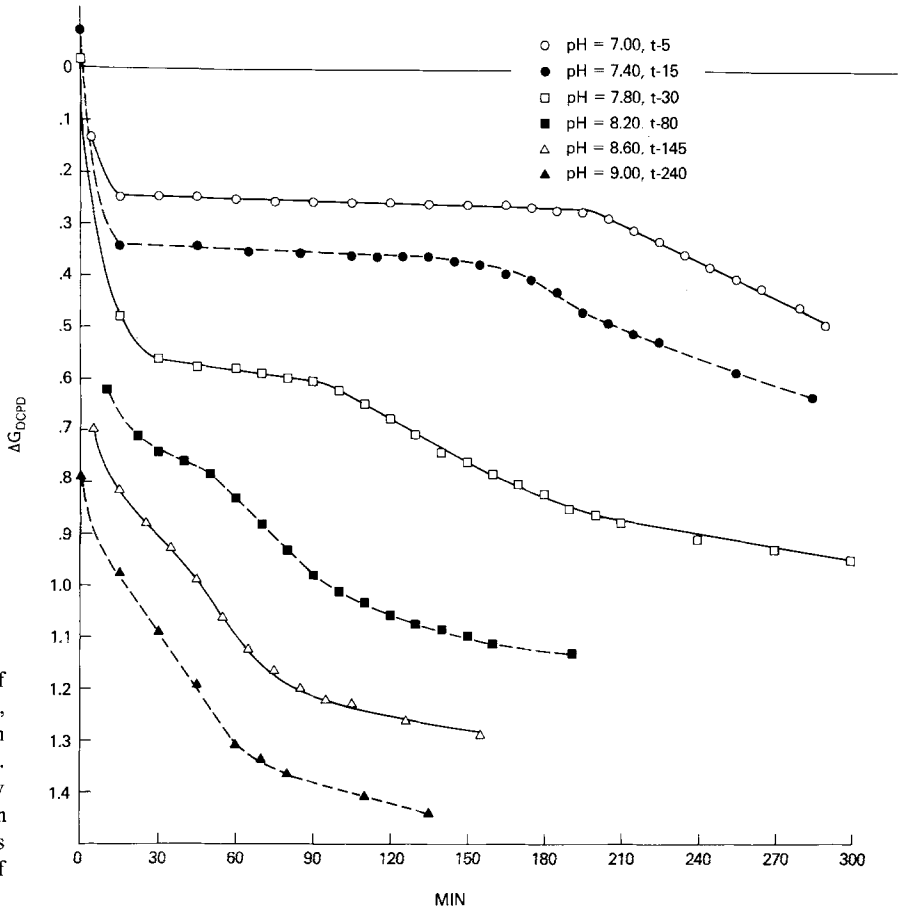

Fig. 8. The thermodynamic stability of solutions of pH 7.00, 7.40, 7.80, 8.20, 8.60, and 9.00 compared to solutions in equilibrium with pure crystalline DCPD. The data encompass only the secondary transition stage. The time axis has been adjusted by subtracting the indicated times (in min) corresponding to the duration of the amorphous–crystalline transition

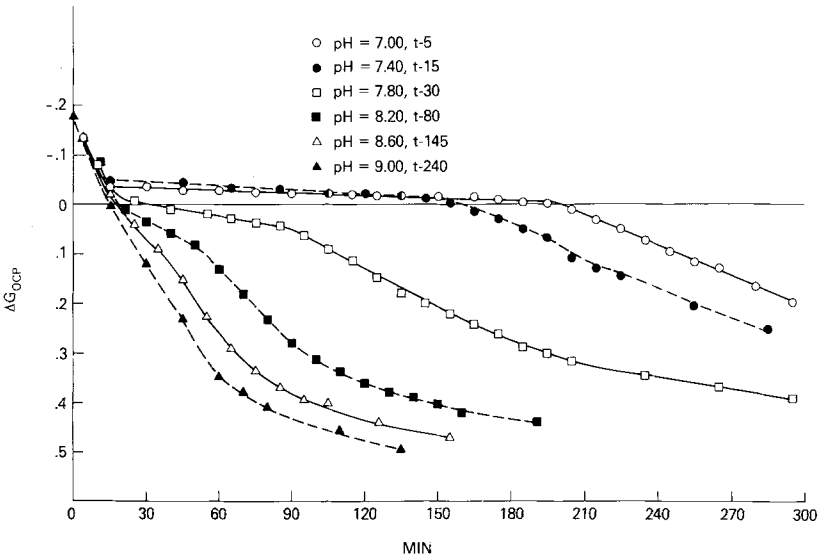

Fig. 9. The thermodynamic stability of solutions of pH 7.00, 7.40, 7.80, 8.20, 8.60 and 9.00 compared to solutions in equilibrium with pure crystalline OCP. The data encompass only the secondary transition stage. The time axis has been adjusted by subtracting the indicated times (in min) corresponding to the duration of the amorphous–crystalline transition

respectively, of the flat portion of the curves following the amorphous–crystalline transformation. The times were obtained from the kinetic plots as the intersection of tangents to each of the sharp breaks in the curve, immediately preceeding and following the flat portion of the curve, with an essentially straight line drawn through all the points taken during this period. The Δt values indicate the time periods during which the

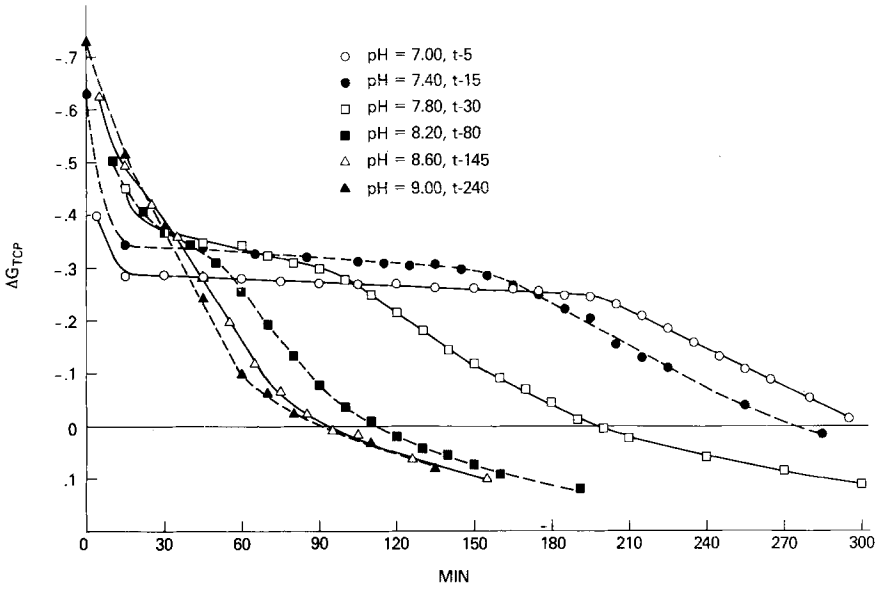

Fig. 10. The thermodynamic stability of solutions of pH 7.00, 7.40, 7.80, 8.20, 8.60, and 9.00 compared to solutions in equilibrium with pure crystalline TCP. The data encompass only the secondary transition stage. The time axis has been adjusted by subtracting the indicated times (in min) corresponding to the duration of the amorphous–crystalline transition

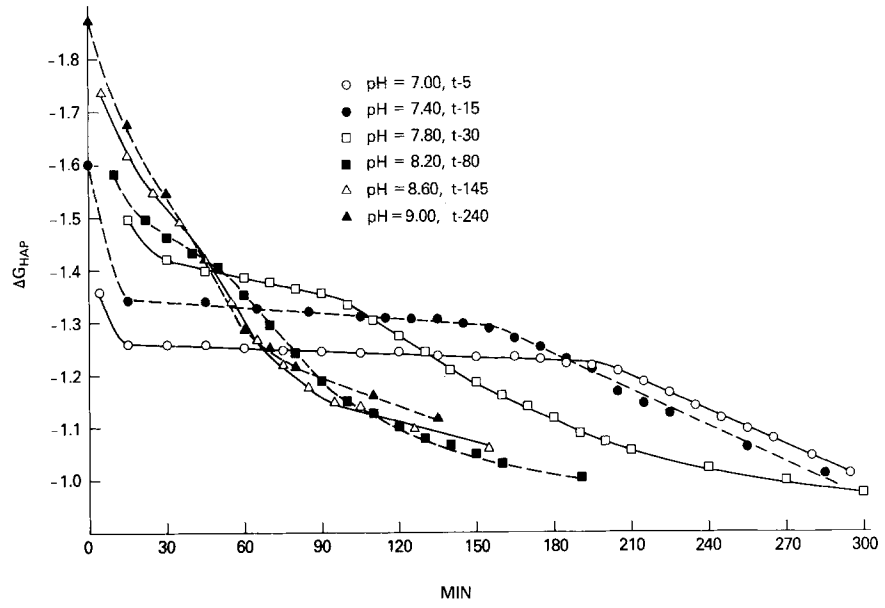

Fig. 11. The thermodynamic stability of solutions of pH 7.00, 7.40, 7.80, 8.20, 8.60, and 9.00 compared to solutions in equilibrium with pure crystalline HAP. The data encompass only the secondary transition stage. The time axis has been adjusted by subtracting the indicated times (in min) corresponding to the duration of the amorphous–crystalline transition

secondary phase was present at each of the values of pH. It can be seen that these values decreased with increasing pH. In fact, at pH 8.80 and 9.00, the secondary phase became so unstable that accurate estimates of Δt could not be obtained and are not included in Table 1. ΔG values, in kcal/mol, were calculated for the solution composition, with respect to equilibrium with the solid phase, DCPD, OCP, TCP, and HAP, which existed at each of the time points listed in the Table. The subscripts B and A, respectively, signify the free energy of the solution before and after the flat portion of the curves. It is to be noted that, whereas the ΔG values for OCP at the beginning of the secondary stage are invariant with respect to pH, at the end of this stage only the ΔG values for TCP show little variation with pH.

Discussion

The data collected from solutions in this study show the existence of a secondary inflection in solubility following the amorphous to crystalline transformation. Crystalline material isolated during this secondary stage differs significantly from the subsequent apatitic

Table 1. Free energy and induction period parameters for the secondary calcium phosphate transition stage[a]

pH	t_B	t_A	Δt	DCPD		OCP		TCP		HAP	
				ΔG_B	ΔG_A	ΔG_A	ΔG_A	ΔG_B	ΔG_A	ΔG_B	ΔG_A
7.00	10	203	193	0.25	0.27	−0.04	−0.01	−0.29	−0.25	−1.26	−1.22
7.20	14	184	170	0.32	0.34	−0.04	−0.01	−0.32	−0.28	−1.31	−1.27
7.40	25	177	152	0.34	0.37	−0.05	−0.01	−0.34	−0.29	−1.34	−1.29
7.60	33	136	103	0.48	0.52	−0.02	0.03	−0.36	−0.29	−1.38	−1.32
7.80	47	127	80	0.55	0.61	−0.02	0.05	−0.39	−0.29	−1.43	−1.34
8.00	63	122	59	0.61	0.69	−0.03	0.06	−0.42	−0.31	−1.49	−1.38
8.20	93	135	42	0.69	0.80	−0.01	0.10	−0.44	−0.30	−1.52	−1.39
8.40	124	163	39	0.74	0.88	−0.02	0.13	−0.48	−0.29	−1.58	−1.40
8.60	154	186	32	0.79	0.96	−0.05	0.13	−0.53	−0.31	−1.66	−1.46

[a] Subscripts B and A signify conditions of time, t, in min and free energy, ΔG, in kcal/mol before and after, respectively, the secondary transition stage

phase (Eanes and Meyer, 1977). Some information on the structure and identity of the first-formed crystalline phase can be inferred by examining the thermodynamic stability of the solutions in equilibrium with the solid phase.

First, the existence of DCPD or a DCPD-like phase in the first-formed crystalline material can be ruled out on the basis of the information presented in Figures 4 and 8. Under all conditions during the secondary transition the solution phase is undersaturated with respect to DCPD (ΔG positive). Also the flat portions of the curves are greatly displaced along the ΔG axis, with the variation in pH of the solution, indicating that an ion activity product of the type (Ca^{2+}) (HPO_4^{2-}) varies with solution conditions. Thus even a hypothetical less soluble calcium phosphate phase with a $CaHPO_4$ composition is unlikely as an intermediate phase, since a consistent ion product was not obtained.

A similar type of argument rules out the existence of a pure HAP-like phase in the first crystallized material. The metastable phase is formed under conditions at which the solution is highly unstable with respect to HAP (ΔG negative) as indicated by the results in Figures 7 and 11. It seems unlikely that a metastable apatitic phase would form with a thermodynamic stability so different from HAP. The ion product for the solution phase, considering HAP as the appropriate molecular formula, also varies with pH as indicated by the Figures. The variability of the ion product with pH is more clearly seen in Table 1. The calculated ΔG values, both before and after the secondary transformation, become progressively more negative as the pH increases. This is in contrast to the solution ΔG values which refer to a DCPD solid phase which become more positive as the pH increases.

The situation becomes more interesting when we consider the stability of the solution phases with respect to OCP and TCP, however. The conclusion that is immediately drawn, when Figures 5 and 9 are examined, is that the solution phase in equilibrium with the first-formed crystalline phase has a thermodynamic stability very similar to that of OCP. The ΔG curves begin to flatten at a point very near to but slightly above the $\Delta G = 0$ line. The lines are initially nearly superimposable, and the flat portion of the post-amorphous–crystalline transformation curves remains near the $\Delta G = 0$ line until the secondary transformation takes place under the conditions at which the secondary phase is most stable (pH $\leq$7.8). The ΔG values in Table 1 indicate that the ion activity product for OCP for the solution phase in contact with the first-formed crystalline material is invariant and nearly identical with the reported solubility product for OCP. The average value for ΔG_B for the 9 experiments in Table 1 is −0.03 kcal/mol with a range of $\pm$0.02. A log solubility product of −47.14 is calculated from these data, compared to the literature value of −47.33. This indicates a crystalline phase with only a slightly greater solubility than well crystallized OCP. This seems reasonable since freshly formed crystals generally have somewhat greater solubilities than mature crystals. On the other hand, the observation that the ΔG_A values for OCP are dependent upon the solution condition suggests that OCP is no longer present in the solid phase at the end of the secondary phase transformation.

The ΔG curves, Figures 6 and 10, which describe the solution conditions with respect to TCP yield little information upon inspection since there is no obvious correlation with the $\Delta G = 0$ line, nor is there a great dependence of the flat portion of the plots on solution pH. Examination of Table 1, however, reveals an interesting relationship between the TCP ion product and the solution phase in equilibrium with solid phase. Although the ΔG_B values become more negative as the

pH is increased, the ΔG_A values show little variation with pH. This indicates that at the end of the secondary transition period the solution is in equilibrium with a calcium phosphate phase with a molecular composition similar to $Ca_3(PO_4)_2$. The average ΔG value for this TCP ion product is −0.29 kcal/mol with a range of ±0.04. The log solubility product calculated for this, perhaps hypothetical $Ca_3(PO_4)_2$ phase, is −27.80. The consistency of this ion product at the end of the secondary transition stage suggests that there is little, if any, hydroxide in the crystal lattice.

The results of the thermodynamic analysis of the data obtained from solutions in equilibrium with the solid phases during the secondary transition strongly suggest that OCP is present in the first-formed crystalline phase and governs the solubility of that phase. The data further suggest that, during the secondary transformation, OCP hydrolyzes to a more basic calcium phosphate. The calculations suggest that crystalline material present at the end of this transformation has a TCP-like composition. Based on earlier X-ray studies, this phase undoubtedly has an apatitic structure (Eanes and Meyer, 1977). It is speculated that the further maturation of this phase to HAP consists of the incorporation of calcium and hydroxide ions into this post-secondary transformation phase. The previous inability to detect OCP by diffraction methods in the first-formed crystalline calcium phosphate has been explained (Eanes and Meyer, 1977).

The kinetic results obtained in this, and in an earlier investigation, support the proposed sequence of events that occur immediately after the amorphous–crystalline transformation. First, the only adequate explanation of the dependence of the stability of the amorphous phase on solution composition requires that OCP is the first nucleated crystalline calcium phosphate phase in the amorphous–crystalline transformation (Meyer and Eanes, in press). The kinetic results of this study also suggest that an acidic phase is present in the first-formed crystalline phase. As the pH is increased the stability of this phase rapidly decreases as seen by the Δt values in Table 1. It requires 193 min for the secondary transformation to take place at pH 7.00 while the transformation is too rapid for an accurate measurement at pH ≥8.80. This dependence on pH is highly suggestive of a transformation of an acidic to a more basic compound.

The balanced chemical reaction (1) describes the overall sequence that would occur in the secondary transformation as proposed above.

$$5Ca_4H(PO_4)_3 + Ca^{2+} + 4OH^- \rightarrow 7Ca_3(PO_4)_2 + HPO_4^{2-} + 4H_2O \quad (1)$$

This reaction requires an uptake of calcium and hydroxide ions from solution and the possibility, if Reaction 1 occurs more rapidly than the overall removal of calcium and phosphate from solution, of an increase in solution phosphate. Calcium and hydroxide uptake has been noted at all times under all conditions and an increase in solution phosphate is often observed if the conditions are correct as in Figures 2 and 3. The further development of the apatitic phase from a $Ca_3(PO_4)_2$ composition to the stoichiometry of HAP would follow reaction scheme (2).

$$8Ca_3(PO_4)_2 + Ca^{2+} + 4OH^- + H_2O \rightarrow 5Ca_5(PO_4)_3OH + HPO_4^{2-} \quad (2)$$

The latter equation also requires the consistent removal of calcium and hydroxide ions and the possible addition of phosphate ions to solution. This has also been verified by experiments as is noted in the immediate post-secondary transformation results in Figures 2 and 3.

References

Betts, F., Posner, A.S.: An x-ray radial distribution study of amorphous calcium phosphate. Mat. Res. Bull. **9**, 353–390 (1974)

Boskey, A.L., Posner, A.S.: Conversion of amorphous calcium phosphate to microcrystalline hydroxyapatite. A pH-dependent, solution-mediated, solid–solid conversion. J. Phys. Chem. **77**, 2312–2317 (1973)

Eanes, E.D., Meyer, J.L.: The maturation of crystalline calcium phosphates in aqueous suspensions at physiological pH. Calcif. Tiss. Res. **23**, 259–269 (1977)

Eanes, E.D., Posner, A.S.: Kinetics and mechanism of conversion of noncrystalline calcium phosphate to crystalline hydroxyapatite. Trans. N.Y. Acad. Sci. **28**, 233–241 (1965)

Gregory, T.M., Moreno, E.C., Brown, W.E.: Solubility of $CaHPO_4 \cdot 2H_2O$ in the system $Ca(OH)_2$–H_3PO_4–H_2O at 5, 15, 25, and 37.5° C. J. Res. Natl. Bur. Stand. **74A**, 461–475 (1970)

Gregory, T.M., Moreno, E.C., Patel, J.M., Brown, W.E.: Solubility of β-$Ca_3(PO_4)_2$ in the system $Ca(OH)_2$–H_3PO_4–H_2O at 5, 15, 25, and 37° C. J. Res. Natl. Bur. Stand. **78A**, 667–674 (1974)

McDowell, H., Wallace, B.M., Brown, W.E.: The solubilities of hydroxyapatite at 5, 15, 25, and 37° C, abstracted, IADR Program and Abstracts of Papers, No. 340 (1969)

Meyer, J.L., Eanes, E.D.: A thermodynamic analysis of the amorphous to crystalline calcium phosphate transformation. Calcif. Tiss. Res. (in press)

Moreno, E.C., Brown, W.E., Osborn, G.: Stability of dicalcium phosphate dihydrate in aqueous solutions and solubility of octacalcium phosphate. Soil Science Society of America Proceedings **21**, 99–102 (1960)

Murphy, J., Riley, J.P.: A modified single solution method for the determination of phosphate in natural waters. Anal. Chim. Acta **27**, 31–36 (1962)

Nancollas, G.H., Tomazic, B.: Growth of calcium phosphate on hydroxyapatite crystals. Effect of supersaturation and ionic medium. J. Phys. Chem. **78**, 2218–2225 (1974)

Termine, J.D., Eanes, E.D.: Comparative chemistry of amorphous and apatitic calcium phosphate preparations. Calcif. Tiss. Res. **10**, 171–197 (1972)

Received July 25 / Revised December 1 / Accepted December 5, 1977